Original Research Article: full paper

(2023), «EUREKA: Physics and Engineering»
Number 5

ENERGY LOSSES STUDY IN SOLAR HYBRID GAS TURBINE IN COLOMBIA

Faustino Moreno-Gamboa✉
Department of Mechanical Engineer[1]
faustinomoreno@ufps.edu.co

Gustavo Guerrero-Gomez
Department of Mechanical Engineer
Francisco de Paula Santander University Ocana Section
Alcosure road, Ocana, Colombia, 546551

Alvaro Jr Caicedo-Rolon
Department of Industrial Engineer[1]

[1]*Francisco de Paula Santander University*
12 e 96, Gran Colombia ave., Cucuta, Colombia, 54003

✉**Corresponding author**

Abstract

Due to decrease of oil reserves, the international commitment for the reduction of pollutant emissions and environmental protection, renewable energy sources are intensively studied, including solar energy applications. However, solar energy is not constant and one possible alternative are solar hybrid thermosolar power plants. A hybrid solar gas turbine has three subsystems: a solar concentrator with heliostat field and central tower receiver, a combustion chamber, and a regenerative gas turbine. A previous thermodynamic analysis allowed shows an energy and exergy study of the plant, from a thermodynamic model of the system that has a method of solar resource estimation. However, this analysis did not allow evaluation of the energy losses in the system components, although the original model considered the typical irreversibilities of these cycles. This work aimed to develop a thermodynamic model that estimates the energy losses in the subsystems and the solar hybrid gas turbine components from a few parameters. The model estimated the energy losses for a Brayton cycle hybrid solar thermal plant throughout the day July 20 in Barranquilla, Colombia. A Dymola compiler in Modelica language was used to evaluate the model, which facilitates the estimation of the results at different times of the day. In this case, the computations were performed hourly throughout the day. In the results, energy losses were 16 % in the solar concentrator when the solar resource was the maximum at noon and close to 1 % in the combustion chamber. Therefore, the hybrid solar Brayton cycle system is technically feasible and reduces fuel consumption. Consequently, it is important to continue developing concentration systems and reduce their energy losses.

Keywords: gas turbine, energy losses, solar concentrator, heliostat field, central tower, energy flows, solar radiation, efficiency, combustion chamber, power plant.

DOI: 10.21303/2461-4262.2023.003108

1. Introduction

Over the past ten years, the energy demand from fossil fuels increased by 1.7 % annually, while the demand for renewable energy, including hydropower and biofuels, increased by 4.4 % annually. However, 80.3 % of the energy consumed comes from fossil fuels [1]. For example, in Colombia, 69 % of the electrical power is generated by hydraulic systems, 29 % by thermal plants using coal and natural gas, and only 0.3 % by renewable sources [2].

Solar energy is an important source of renewable energy. Photovoltaic systems have reached a significant level of technological maturity; however, researchers still seek to develop materials with greater efficiency [3]. Solar radiation can also be concentrated by a relationship between a reflecting surface that receives the direct radiation and concentrates it on a smaller receiving surface. The concentrated energy at the receiver is delivered to a working fluid within a power cycle, defining Concentrating Solar Power (CSP) cycles [4]. Concentrating solar power systems range from a parabolic dish, Fresnel, parabolic trough, and heliostat to central tower field concentrators, the last two being the most developed at present [5].

Although there are several concentrating solar power systems, the most developed are the parabolic trough and central tower heliostat systems, which have been successfully applied in steam cycles with and without thermal storage [6]. An application under development focuses on coupling CSP systems with gas turbines, which can operate in several configurations and power ranges, making them very versatile in terms of location and type of application [7, 8].

Gas turbines can generate more power by increasing the maximum temperature of the cycle. However, the solar resource is not constant, which is a challenge that can be solved by hybridization with a combustor that keeps the turbine inlet temperature as high and stable as possible, even when the solar resource is not available [9]. Hybrid gas turbine systems with heliostat field solar concentrators and central towers are not commercially available except for small models up to 100 kW [10]. However, experimental designs in investigation and development confirm that the technology is technically feasible [11, 12]. Hybrid CSP systems with gas turbines still require important work in the coupling and control of the hybrid heat supply system with the power cycle [13], the solar receiver [14], and the use of combined cycles [7]. Moreover, the possibility of using different working fluids, such as carbon dioxide, in supercritical conditions can generate significant advances for its high efficiency due to the low work required by the compressor [15, 16].

The northern region of Colombia has the potential to develop concentrating solar thermal systems [17]. Then, it is important to evaluate the operation of these systems in this region and contribute to the search for new energy sources that allow diversifying Colombia's energy basket.

The main goal of this work is to evaluate the energy losses and flows of a solar hybrid Brayton cycle power plant with a heliostats field concentration system and receiver in a central tower. In the development of the work, the following objectives are met. First, develop a model for estimates the energy losses and flows in the different components of the plant subsystems during an average day of the year. Second, the plant operation is evaluated in Barranquilla, Colombia, using its climatic conditions and the parameters of a plant called Solugas in Spain.

2. Materials and methods

2. 1. Object of the study

A crucial parameter in evaluating concentrating solar power systems is the availability of information on direct solar radiation at a particular place, ideally from reliable long-term measurements [4]. However, many countries like Colombia have no robust infrastructure to measure and process solar radiation data over large areas. In this sense, researchers have developed models to estimate solar resources in different locations and days of the year, such as the Daily Integration (DI) model developed by [18]. The DI model is considered the most accurate after being compared with measured data and results from similar models at different locations [19, 20].

It is necessary to evaluate the energy losses in the hybrid solar turbine and develop a model for estimates the energy losses and flows in the different components of the plant subsystems during an average day of the year. The plant operation is evaluated in Barranquilla, Colombia, using its climatic conditions.

2. 2. Solar model

In the DI model, the total irradiance on a horizontal surface, I_h, is the sum of its components, the direct irradiance, I_{bh}, and the diffuse irradiance, I_{dh}. Therefore, direct radiation is shown in equation (1):

$$I_{bh} = I_h - I_{dh}. \tag{1}$$

To distribute values during the day, let's present below the hour-to-day relations for diffuse r_d and global r_t radiation, according to equations (2) and (3):

$$r_d = I_{dh} / D_h, \tag{2}$$

$$r_t = I_h / H_h, \tag{3}$$

D_h and H_h represent the long-term monthly average daily value for total and diffuse radiation found at the National Aeronautics and Space Administration [21]. Equation (4) express Direct radiation as a function of the time of day and global and diffuse radiation:

$$I_{bh} = r_t H_h - r_d D_h. \tag{4}$$

2. 3. Thermodynamic model of energy losses

This research considered a hybrid Brayton cycle solar plant (**Fig. 1**) shows the scheme, and **Fig. 2** displays the diagram where the plant's main subsystems and energy flows. The plant has three subsystems. The first is a solar concentration subsystem with a central tower and a heliostat field. The second is a combustion chamber that consumes natural gas to complete the energy supply required by the third subsystem, defined as the power cycle.

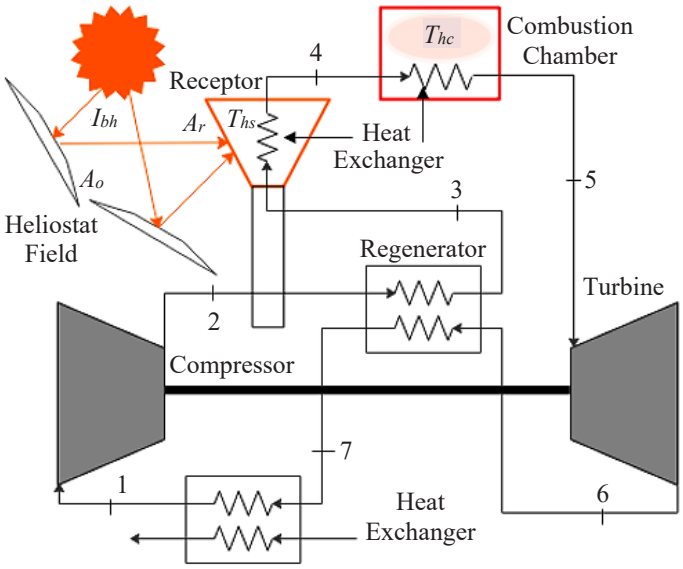

Fig. 1. Schematic of the Brayton Cycle Hybrid Solar Power plant

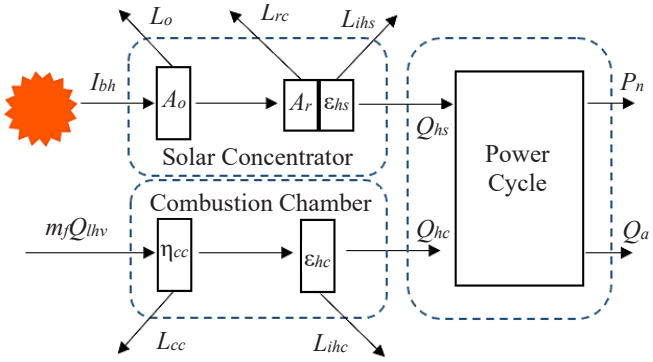

Fig. 2. Power plant energy flows

In [22, 23] has been presented a detailed thermodynamic model of a hybrid solar Brayton cycle power plant operation. Based on this model, the energy flows are shown below, including energy losses in the different components of the plant. The description of the energy flows and the variables in **Fig. 2** are described below. In the solar concentrator, the heliostat field of the area A_o receives direct solar radiation (**Fig. 1, 2**). Therefore, the energy flow entering the plant through the solar concentrating system is defined by the equation (5):

$$Q_{is} = I_{bht} A_o. \tag{5}$$

The heliostat field is characterized by its optical efficiency (η_o), defined as a function of blocking and shadowing, intersection, mirror, cosine, and atmospheric effects.

However, using constant average values to analyze the concentration system is possible, according to [13, 24], which allows defining energy losses in the heliostat field (L_o), by equation (6):

$$L_o = I_{bh} A_o \left(1 - \eta_o\right). \tag{6}$$

The receiver area (A_r) concentrates the energy flow from the heliostat field. This area contains the receiver losses (L_{rc}), including conduction and convection losses, which a single coefficient can summarize U_l, as shown in the first term of equation (7) [25]. In addition, the receiver presents losses by radiation described in the second term of equation (7), where α is the receiver emissivity, σ is the Stefan-Boltzmann constant, and T_{hs} and T_o are the receivers and room temperatures, respectively:

$$L_{rc} = U_l A_r \left(T_{hs} - T_o\right) + \alpha\sigma A_r \left(T_{hs}^4 - T_o^4\right). \tag{7}$$

In the tower receiver, the fluid receives energy through a heat exchanger characterized by its efficiency ε_{hs}, so the fraction of energy lost is multiplied by the heat entering the heat exchanger, Energy lost in the heat exchanger (L_{ihs}) of the solar receiver as seen in the equation (8):

$$L_{ihs} = \left(I_{bh} A_o - I_{bh} A_o \left(1 - \eta_o\right) - L_{rc}\right) * \left(1 - \varepsilon_{hs}\right). \tag{8}$$

Regarding the combustion chamber, the energy input (Q_{ic}) with the fuel can be defined as a function of lower heating value (Q_{lhv}) and the mass flow of the fuel (m_f) (see equation (9)):

$$Q_{ic} = Q_{lhv} m_f. \tag{9}$$

Considering that the efficiency η_{cc} defines the combustion, and equation (10) estimates the losses in combustion process (L_{cc}) is:

$$L_{cc} = Q_{lhv} m_f (1 - \eta_{cc}). \tag{10}$$

In the combustion chamber, the working fluid receives energy through a heat exchanger characterized by efficiency (ε_{hc}). In this sense, equation (11) estimates the energy lost in the combustion chamber heat exchanger:

$$L_{ihc} = (Q_{lhv} m_f - Q_{lhv} m_f (1 - \eta_{cc})) * (1 - \varepsilon_{hc}). \tag{11}$$

The energy entering the system through the solar concentrator and combustion chamber is estimated by equation (12):

$$Q_{iT} = Q_{ic} + Q_{is} = m_f Q_{lhv} + I_{bh} A_o. \tag{12}$$

The thermal engine receives a total energy Q_h, which is the heat that the working fluid (m) gets, represented by the sum of the heat delivered in the combustion chamber Q_{hc} and in the solar concentrator Q_{hs} (13). Where (h) is the enthalpy in each state:

$$Q_h = Q_{hc} + Q_{hs} = m\left(h_5 - h_4\right) + m\left(h_4 - h_3\right). \tag{13}$$

The power output of solar hybrid power plant, P_n, is evaluated by equation (14):

$$P_n = m\left(h_5 - h_6\right) + m\left(h_2 - h_1\right). \tag{14}$$

Equation (15) shows the overall efficiency power plant (η), It is the relationship between power and the total energy entering the plant:

$$\eta = P_n / Q_{in}. \tag{15}$$

In addition, the cycle dissipates heat into the environment, Q_a, through a heat exchanger [9, 13], which is expressed in equation (16):

$$Q_a = m(h_7 - h_1). \tag{16}$$

The model in general is ideal for a pre-design stage of this plants, at another level detailed engineering is required to complete the design. The concentration model is simple and does not take into account the variation in optical efficiency, but it is useful in the preliminary analysis of the use of solar energy.

3. Results and discussion

This section first presents the validation of the solar radiation estimation model and the thermodynamic model of the plant. Then, it describes the plant's operation results on an average year's day, and the energy flows in the cycle. Next, let's use the Dymola compiler in Modelica language to validate and simulate the models considering the city's annual average D_h and H_h and hourly average temperature values [26]. Finally, [22] present the model details, validation, and simulation parameters.

The data is collected from Meteosevilla on July 20, Spain, to validate the solar radiation model (DI model), and considered the global radiation of $H_h = 7.8$ kWh/m^2/day and the diffuse radiation of $D_h = 1.7$ kWh/m^2/day [21]. The latitude of the place is 37.38° North. Then, let's compare the results from the DI model with the data from Meteosevilla using the Mean Absolute Bias Error (MABE) and the Root Mean Square Error (RMSE). Finally, let's obtain a MABE of 0.2010085 and an RMSE of 0.226616, which are acceptable according to [19, 20].

Table 1 compares the model results with data from the manufacturer of the Mercury 50 turbine [27] for the power (P_n) and the overall plant efficiency (η) with the Solugas project results [9], obtaining maximum errors of 0.7 %, indicating a good correlation of model.

Table 1
Validation of the thermodynamic model

Item	P_n (kW)	η
Model	4,635.4	0.302
Reference	4,600 [27]	0.300 [9]
Error %	0.7	0.66

Considering that the plant's primary function is to generate electricity, **Fig. 3** shows the variation of the plant's output during an average day of the year (June 20) in Barranquilla, Colombia, given its location and environmental conditions [26]. The results indicate that the power variation is low since its relative amplitude is 3 % during the day and is not affected by the inclusion of the solar concentration system. The above is because the power is subordinated to the combustion chamber temperature, which is constant, and to the ambient temperature variations [28]. In addition, **Fig. 3** also presents the evolution of the plant's overall efficiency during the day. This picture shows that the trend of η is also opposite to the ambient temperature when there is no solar resource. However, when the solar concentrating system contributes energy to the cycle, the overall efficiency decreases due to concentrator losses, generating a maximum decrease in η of 14.2 %.

Let's present the solar concentrator's energy flows because of the influence of energy losses on the system's overall efficiency. First, **Fig. 4** shows the energy received by the heliostat field (Q_{is})

and the energy delivered to the power cycle (Q_{hs}), representing an efficiency of 55.6 % at noon, including optical losses (heliostats) in the receptor and the receiver heat exchanger.

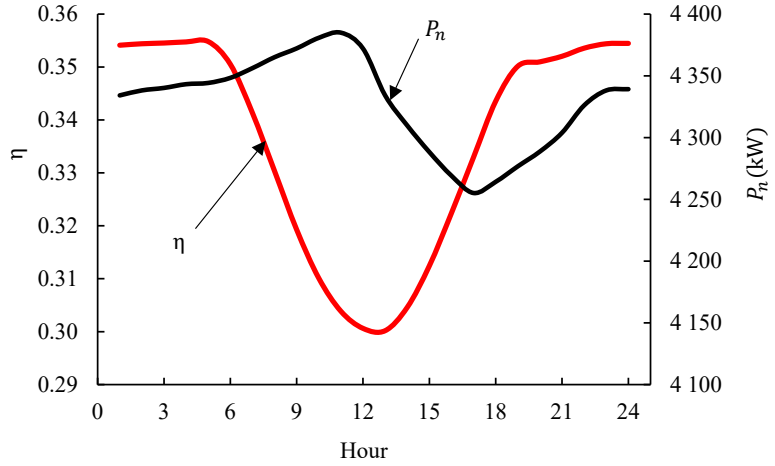

Fig. 3. Evolution of power and overall plant efficiency

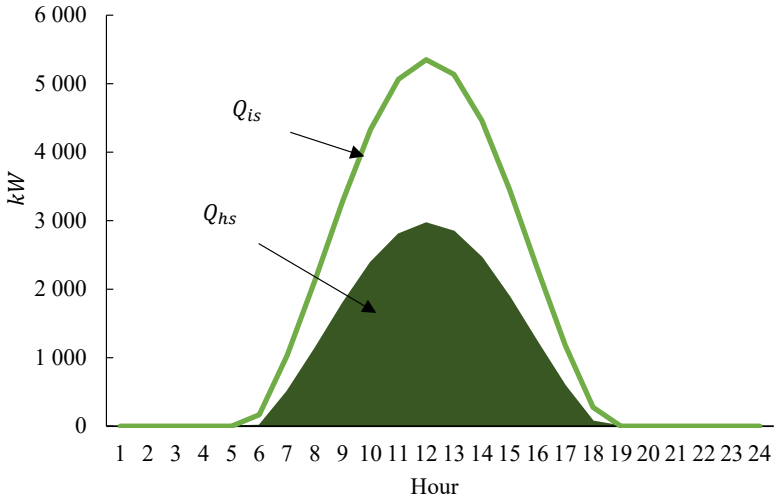

Fig. 4. Total energy entering the solar concentrator and energy supplied to the power cycle

Fig. 5 displays the variation of the energy losses in the heliostat field (L_o) that reach a maximum value of 1,444 kW at noon and represent a fraction of 0.093 concerning Q_{iT}. The energy losses in the heliostat field are a function of the optical efficiency (η_o), which is a function of blockage and shadowing, the effect of intersections, mirror selectivity, and cosine and atmospheric effects. However, this research considered the average values used in the literature ($\eta_o = 0.73$) [29]. Furthermore, the losses in the solar receiver, L_{rc}, are non-linear (see equation (7)) and reach a maximum value of 200.7 kW at midday and a fraction of 0.015 of Q_{iT}. Finally, the receiver heat exchanger losses (L_{ihs}) are a function of the exchanger efficiency ε_{hs}, reaching a maximum value of 741 kW at noon and representing a fraction of 0.051 of the total energy entering the system.

When direct solar radiation increases during the day, energy losses in the solar concentrator increase due to the increase in heat transfer and the increase in temperature in the solar receiver. In the evaluation, values of optical efficiency and solar receptor heat exchanger effectiveness in particular cases were used, although in other cases lower values have been used with the respective increase in energy losses in the solar concentrator [28].

The combustion chamber is the second energy source for the power cycle. **Fig. 6** presents the energy entering the combustor related to the lower heating value of the fuel (Q_{ic}) and the

energy delivered to the power cycle (Q_{hc}), with an efficiency of 96 %. The above makes sense because the combustion efficiency is ($\eta_{cc} = 0.98$), and the efficiency of the heat exchanger in the combustor is ($\varepsilon_{cc} = 0.98$). Therefore, the curve dip of **Fig. 6** represents the fuel consumption savings, with a saving of about 7.6 % during the day since this energy is supplied by the solar concentrator.

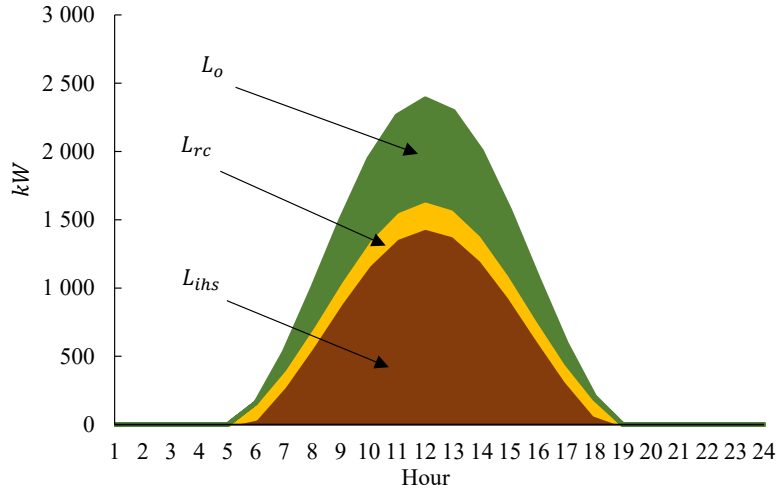

Fig. 5. Energy losses in the solar concentrator

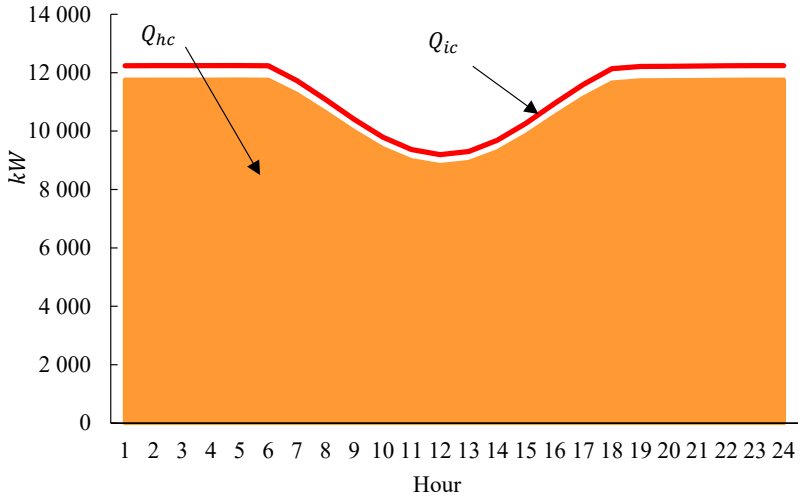

Fig. 6. Energy losses in the solar concentrator

Fig. 7 displays the heat losses in the combustion process (L_{cc}) and in the combustion chamber heat exchanger (L_{ihc}), which, concerning Q_{iT}, represent a fraction of 0.037 and 0.014, respectively, when the contribution of the solar concentration system is maximum at noon. The hybridization system through the combustion chamber regulates the operation of the plant and controls the fuel supply to ensure a near-constant power output. Additionally, the combustion chamber allows the turbine inlet temperature to be regulated and the power output to be controlled, when the solar concentration system provides energy. Energy losses are associated with the efficiency of the combustion process and the effectiveness of the heat exchanger.

Fig. 8 compares the energy flows in the plant's three main subsystems, where the red line represents the total energy input Q_{iT}, showing that despite reducing fuel consumption with the solar contribution, it also increases the total energy input to the system, reaching a maximum of 14,543 kW at midday. The green area represents the energy lost in the solar concentrator, whose details are in **Fig. 5**, corresponding to a fraction of 0.16 of Q_{iT} at noon.

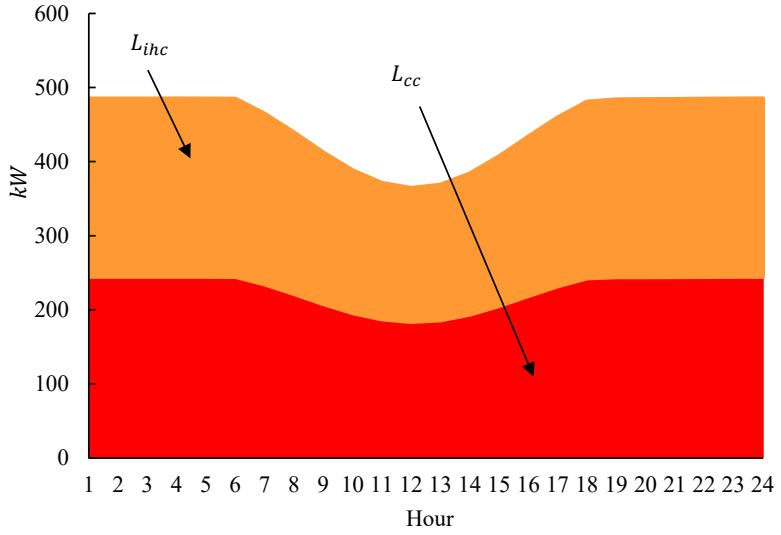

Fig. 7. Energy losses in combustion chamber

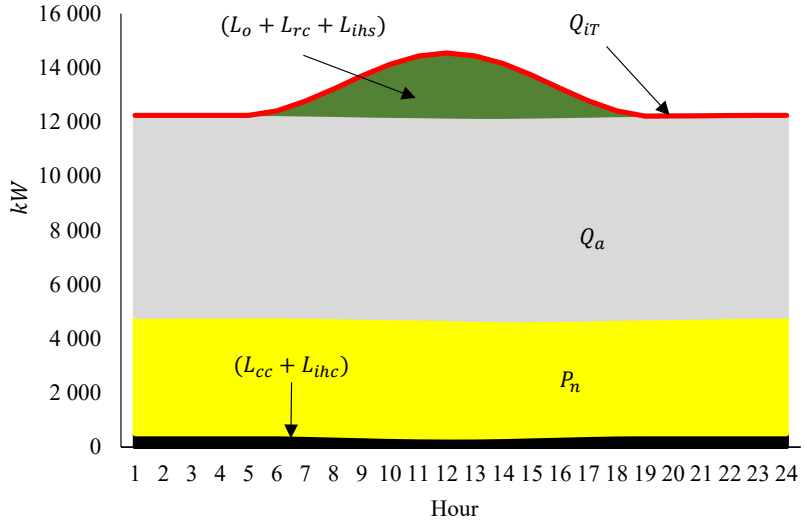

Fig. 8. Total energy input to the system and total energy flows

The energy dissipated in the heat exchanger to the environment is almost constant during the day. However, because of the input energy variation, it is a fraction of 0.51 at noon and 0.58 average at night hours concerning the total energy input. Therefore, the above proves that using heat recovery systems for a particular application or lower supercritical carbon dioxide or organic Rankine cycles (ORC) in this specific system is feasible.

The plant's average power during the day is 4,328 kW (**Fig. 8**). Despite the variations in the solar resource, the variation in power output is only 2.9 % due to the control of the combustion chamber on the turbine inlet temperature (**Fig. 1**). However, the fraction of power varies concerning Q_{iT}. It represents the system's overall efficiency (**Fig. 3**), which decreases with the start-up of the solar concentrating system because of the energy losses of the latter. Furthermore, the loss fraction in the combustion chamber is minimal and varies from 0.079 to 0.051 between night and noon.

The blue line of **Fig. 9** represents the total energy flow entering the power cycle Q_h, with a daily average value of 11,758 kW and a relative variation of 0.6 %. The red area means the energy supplied to the cycle by the combustion chamber Q_{hc}. **Fig. 9** shows that as solar resource becomes available, the energy supplied by the solar concentrator (orange) replaces part of Q_{hc}, reaching a maximum replacement at noon with a supplied energy of 2,963 kW when solar radiation is maximum, replacing 25.1 % of the total energy entering the power cycle. The energy supplied by the

solar concentrator depends on direct solar radiation, the dimensions of the concentrator and its operating parameters, which is why it requires important control elements, added to the difficulty of concentrating the radiation in an uncontrolled environment.

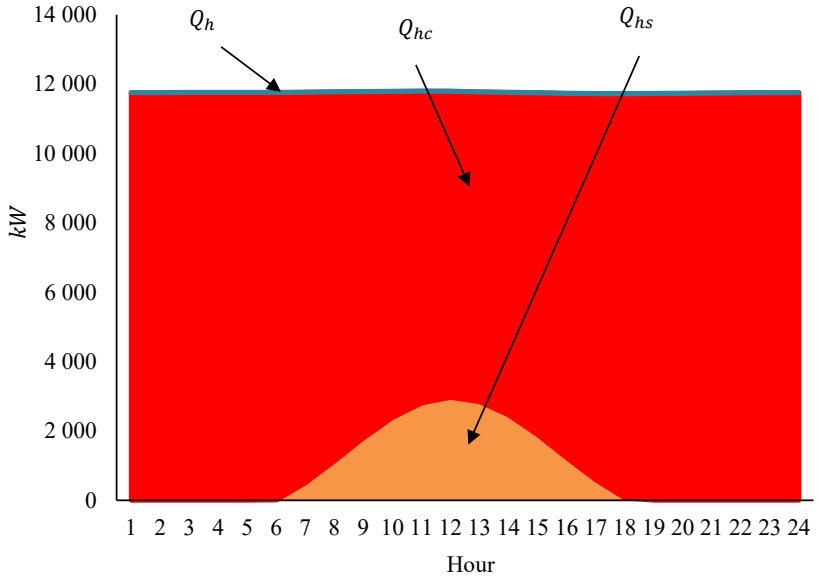

Fig. 9. Total energy entering the power cycle and supplied by the solar concentrator and combustion chamber

Hybrid solar gas turbine systems are still in the development phase with several systems created in experimental centers such as Solugas and PSA in Spain or Sciro in Australia. Among its advantages is the possibility of operating in different configurations and a wide range of powers, as well as its reduced need for water. These solar concentration systems can be coupled to operating plants.

4. Conclusions

Heat losses in the combustion chamber are a function of fuel consumption. Despite being the largest energy source supplied to the turbine, its losses barely reach 2.5 % at noon, including the heat exchanger in the chamber. The above is because fuel consumption, like power, is inversely proportional to ambient temperatures.

The energy entering the solar concentrator is small compared to that entering the combustion chamber, due to the reduced size of the solar field, for the configuration evaluated with the parameters of the Solugas plant. However, the losses in relative terms are much higher for the solar subsystem, including the tower receiver heat exchanger, since this represents the optical losses and is approximately 16 % of the total energy input to the plant when radiation is at its maximum. This research used a simple model for the concentrator. Nevertheless, a detailed analysis of the heliostat field distribution and the losses involved in solar tracking is desirable in future work.

Finally, the heat dissipated to the environment represents an essential fraction of the energy entering despite having a regenerator. Therefore, the previous could facilitate the evaluation of mechanisms to take advantage of this available heat in applications such as lower cycles.

Conflict of interest

The authors declare that they have no conflict of interest in relation to this research, whether financial, personal, authorship or otherwise, that could affect the research and its results presented in this paper.

Financing

The study was performed without financial support.

Data availability

Manuscript has no associated data.

Acknowledgments

The authors acknowledge to Francisco de Paula Santander University for allowing the Dymola license.

References

[1] Renewables 2021, Global Status Report (2021). REN 21. Available at: https://www.ren21.net/wp-content/uploads/2019/05/GSR2021_Full_Report.pdf

[2] Acolgen, la buena energía. Available at: https://acolgen.org.co/

[3] Dimri, N., Tiwari, A., Tiwari, G. N. (2018). Effect of thermoelectric cooler (TEC) integrated at the base of opaque photovoltaic (PV) module to enhance an overall electrical efficiency. Solar Energy, 166, 159–170. doi: https://doi.org/10.1016/j.solener.2018.03.030

[4] Goswami, D. Y. (2022). Principles of Solar Engineering. doi: https://doi.org/10.1201/9781003244387

[5] Nakatani, H., Osada, T. et al. (2012). Development of a Concentrated Solar Power Generation System with a Hot-Air Turbine. Mitsubishi Heavy Industries Technical Review, 49 (1). Available at: https://www.mhi.co.jp/technology/review/pdf/e491/e491001.pdf

[6] Behar, O. (2018). Solar thermal power plants – A review of configurations and performance comparison. Renewable and Sustainable Energy Reviews, 92, 608–627. doi: https://doi.org/10.1016/j.rser.2018.04.102

[7] Jamel, M. S., Abd Rahman, A., Shamsuddin, A. H. (2013). Advances in the integration of solar thermal energy with conventional and non-conventional power plants. Renewable and Sustainable Energy Reviews, 20, 71–81. doi: https://doi.org/10.1016/j.rser.2012.10.027

[8] Horlock, J. H. (2003). Advanced Gas Turbine Cycles. Pergamon. doi: https://doi.org/10.1016/B978-0-08-044273-0.X5000-7

[9] Santos, M. J., Merchán, R. P., Medina, A., Calvo Hernández, A. (2016). Seasonal thermodynamic prediction of the performance of a hybrid solar gas-turbine power plant. Energy Conversion and Management, 115, 89–102. doi: https://doi.org/10.1016/j.enconman.2016.02.019

[10] Doron, P. (2020). A high temperature receiver for a solarized micro-gas-turbine. AIP Conference Proceedings. doi: https://doi.org/10.1063/5.0028527

[11] Dunham, M. T., Iverson, B. D. (2014). High-efficiency thermodynamic power cycles for concentrated solar power systems. Renewable and Sustainable Energy Reviews, 30, 758–770. doi: https://doi.org/10.1016/j.rser.2013.11.010

[12] Quero, M., Korzynietz, R., Ebert, M., Jiménez, A. A., del Río, A., Brioso, J. A. (2014). Solugas – Operation Experience of the First Solar Hybrid Gas Turbine System at MW Scale. Energy Procedia, 49, 1820–1830. doi: https://doi.org/10.1016/j.egypro.2014.03.193

[13] Olivenza-León, D., Medina, A., Calvo Hernández, A. (2015). Thermodynamic modeling of a hybrid solar gas-turbine power plant. Energy Conversion and Management, 93, 435–447. doi: https://doi.org/10.1016/j.enconman.2015.01.027

[14] Martín Sánchez, M. (2018). Evaluación técnico económica de centrales solares de torre con receptores de aire presurizado integrados en turbinas de gas. University of Sevilla. Available at: https://idus.us.es/handle/11441/72405

[15] Liu, Y., Wang, Y., Huang, D. (2019). Supercritical CO_2 Brayton cycle: A state-of-the-art review. Energy, 189, 115900. doi: https://doi.org/10.1016/j.energy.2019.115900

[16] Lei, X., Peng, R., Guo, Z., Li, H., Ali, K., Zhou, X. (2020). Experimental comparison of the heat transfer of carbon dioxide under subcritical and supercritical pressures. International Journal of Heat and Mass Transfer, 152, 119562. doi: https://doi.org/10.1016/j.ijheatmasstransfer.2020.119562

[17] Guzman, L., Henao, A., Vasquez, R. (2014). Simulation and Optimization of a Parabolic Trough Solar Power Plant in the City of Barranquilla by Using System Advisor Model (SAM). Energy Procedia, 57, 497–506. doi: https://doi.org/10.1016/j.egypro.2014.10.203

[18] Gueymard, C. (2000). Prediction and Performance Assessment of Mean Hourly Global Radiation. Solar Energy, 68 (3), 285–303. doi: https://doi.org/10.1016/s0038-092x(99)00070-5

[19] Mejdoul, R., Taqi, M. (2012). The Mean Hourly Global Radiation Prediction Models Investigation in Two Different Climate Regions in Morocco. International Journal of Renewable Energy Research-IJRER, 2 (4). Available at: https://www.ijrer.org/ijrer/index.php/ijrer/article/view/316

[20] Yao, W., Li, Z., Xiu, T., Lu, Y., Li, X. (2015). New decomposition models to estimate hourly global solar radiation from the daily value. Solar Energy, 120, 87–99. doi: https://doi.org/10.1016/j.solener.2015.05.038

[21] Power Data Access Viewer. Available at: https://power.larc.nasa.gov/data-access-viewer/

[22] Moreno-Gamboa, F., Escudero-Atehortua, A., Nieto-Londoño, C. (2020). Performance evaluation of external fired hybrid solar gas-turbine power plant in Colombia using energy and exergy methods. Thermal Science and Engineering Progress, 20, 100679. doi: https://doi.org/10.1016/j.tsep.2020.100679

[23] Moreno-Gamboa, F., Escudero-Atehortua, A., Nieto-Londoño, C. (2022). Alternatives to Improve Performance and Operation of a Hybrid Solar Thermal Power Plant Using Hybrid Closed Brayton Cycle. Sustainability, 14 (15), 9479. doi: https://doi.org/10.3390/su14159479

[24] Romero, M., Buck, R., Pacheco, J. E. (2002). An Update on Solar Central Receiver Systems, Projects, and Technologies. Journal of Solar Energy Engineering, 124 (2), 98–108. doi: https://doi.org/10.1115/1.1467921

[25] Duffie, J. A., Beckman, W. A. (2013). Solar Engineering of Thermal Processes. John Wiley & Sons. doi: https://doi.org/10.1002/9781118671603

[26] Ramírez-Cerpa, E., Acosta-Coll, M., Vélez-Zapata, J. (2017). Análisis de condiciones climatológicas de precipitaciones de corto plazo en zonas urbanas: caso de estudio Barranquilla, Colombia. Idesia (Arica), 35 (2). doi: https://doi.org/10.4067/s0718-34292017005000023

[27] Mercury 50. Available at: https://www.solarturbines.com/en_US/products/power-generation-packages/mercury-50.html

[28] Merchán, R. P., Santos, M. J., Reyes-Ramírez, I., Medina, A., Calvo Hernández, A. (2017). Modeling hybrid solar gas-turbine power plants: Thermodynamic projection of annual performance and emissions. Energy Conversion and Management, 134, 314–326. doi: https://doi.org/10.1016/j.enconman.2016.12.044

[29] Romero, M., Steinfeld, A. (2012). Concentrating solar thermal power and thermochemical fuels. Energy & Environmental Science, 5 (11), 9234. doi: https://doi.org/10.1039/c2ee21275g

Received date 23.05.2023
Accepted date 21.09.2023
Published date 29.09.2023

How to cite: *Moreno-Gamboa, F., Guerrero-Gomez, G., Caicedo-Rolon, A. Jr. (2023). Energy losses study in solar hybrid gas turbine in Colombia. EUREKA: Physics and Engineering, 5, 35–45. doi: https://doi.org/10.21303/2461-4262.2023.003108*